A BF_3 FAST NEUTRON DOSIMETER (Long Counter)

by

Walter A. Leyland, Jr.

Thesis submitted to the Graduate Faculty of the
Virginia Polytechnic Institute
in candidacy for the degree of

MASTER OF SCIENCE
in
PHYSICS

September, 1960

Blacksburg, Virginia

TABLE OF CONTENTS

LIST OF FIGURES

LIST OF TABLES

INTRODUCTION

The Cockcroft-Walton accelerator and the UTR-10 reactor at Virginia Polytechnic Institute make available neutron sources ranging in energies from several Kev to 14 Mev. These source facilities present a problem in neutron dosimetry, namely the determination of neutron flux. Since a major difficulty in such a measurement arises from the energy dependent sensitivity of neutron detectors, it is the purpose of this thesis to describe the design, construction, and calibration of a neutron dosimeter for the above energy range in which this dependency is largely eliminated.

The long counter consists of a cylinder of paraffin with a cylindrical thermal-neutron detector along its axis. Fast neutrons impinging upon the face of the counter are degraded to thermal energies by elastic scattering within the paraffin moderator. To establish the dosimeter's response as a function of neutron energy, neutron sources of known yield and energy are used.

THEORY

Qualitative Description

The cross section for neutrons in boron has a $\frac{1}{v}$ dependence up to approximately 100 ev[16]. As a result of this energy dependence, the cross section can be expressed

$$\sigma = \frac{\sigma_t v_t}{v}$$

where σ_t and v_t are the cross section and velocity, respectively, of a neutron with energy 0.0253 ev (thermal).

In a BF_3 detector the contribution to the reaction rate R by neutrons between the energy range E and E+dE in the volume element dV is expressed[17]

$$dR = N(x,y,z)\,\sigma(E)\,\phi(E,x,y,z)\,dE\,dV$$

where N(x,y,z) is the number of B^{10} atoms per unit volume at the point (x,y,z) within the detector, $\sigma(E)$ is the B^{10} cross section at some energy E, $\phi(E,x,y,z)$ is the flux per unit energy interval at the point (x,y,z). Upon integrating throughout the detector volume and over

the neutron spectrum, $0 < E < 100$ ev, the reaction rate is expressed

$$R = \int_V \int_0^{100\,ev} N(x, y, z)\, \sigma(E)\, \phi(E, x, y, z)\, dE\, dV$$

$$= NV \int_0^{100\,ev} \sigma(E)\, \phi(E)\, dE$$

where it is assumed that the flux is independent of position in the detector. If the cross section for boron is substituted in the above expression, then

$$R = NV \sigma_t \nu_t \int_0^{100\,ev} n(E)\, dE$$

$$= NV \sigma_t \nu_t n$$

where n, the number of neutrons per unit volume, is independent of the energy distribution within the limits 0 to 100 ev. By defining the sensitivity of the BF_3 detector as counts per second per unit neutron flux, it follows that

$$\frac{R}{n\nu} = NV \sigma_t \left(\frac{\nu_t}{\nu} \right)$$

or $$\text{Sensitivity} \equiv NV \sigma_t \left(\frac{\nu_t}{\nu} \right)$$

It is evident from the above expression that the sensitivity of a BF_3 detector is independent of the energy of the neutrons measured if the measured neutron velocities, v, approach thermal energy, that is $v=v_t$. In order to establish this condition the detector is enclosed in a moderating media. This implies that the sensitivity is dependent now upon the arrangement of moderating material around the detector.

To obtain a neutron counter having uniform sensitivity for primary source neutrons, a cylindrical arrangement of paraffin surrounding a BF_3 proportional detector is assembled[10,19]. The length of such a counter, being long compared to the mean free path in paraffin of any fast neutron to be detected, gives rise to the designation, "Long Counter."

If fast neutrons impinge upon the face of the counter, they are degraded to thermal energies by elastic scattering collisions in the paraffin. Diffusing into the BF_3 detector, they give rise to n-α reactions with boron. The count rate is determined thus from this

flux of thermal neutrons. If the impinging neutrons are assumed to have an energy spectrum extending from thermal energies up to several Mev, the penetration depth within the paraffin for those neutrons of high energy is great since the mean free path of such neutrons is initially large. When these neutrons reach thermal energies at an appreciable depth from the front face of the counter, their mean free path is reduced and the probability of escape from the front face before detection is small. At the same time, low energy neutrons penetrate the paraffin only a short distance before thermalization and have a correspondingly larger chance of escape through the front face. As a consequence, the detection efficiency for higher energy neutrons is greater than for those neutrons of lower energy.

To increase the low energy contribution to the thermal flux, a modification of the paraffin arrangement is made by drilling eight radial holes in the front face around the BF_3 detector. These holes increase the probability that low energy neutrons will enter the detector.

Effective Source-Counter Distance

To utilize the long counter for relative flux calibration, it is essential to obtain the effective distance between the source and counter. This distance is measured to that point within the paraffin at which the impinging neutrons are considered to be effectively thermalized, thereafter migration to the BF_3 detector is by diffusion. This neutron penetration depth implies that the counter is effectively concentrated at a point which is not the geometric center. This consideration suggests that the long counter behaves as a point detector and thus the count rate, CR, is proportional to the inverse square of the source-counter distance, $d^{(2)}$.

Since the penetration depth is dependent upon the energy of the impinging neutrons, it is necessary to establish this depth in paraffin for each energy group. For counter calibration it is convenient therefore to use a monoenergetic neutron source. The penetration depth, d_o, for the energy group is determined analytically from the intercept of the plot, $(CR)^{-1/2}$ versus d.

Method for Counter Efficiency Computation

The fraction of the total radiation which passes through an aperture is determined by the solid angle subtended by the aperture at the source[12]. If the aperture is identified with the recessed front face of the long counter, the radiation confined within this cone is expressed

$$N = \frac{S}{4\pi (d+d_o)^2} (A\cos\alpha)$$

$$= \frac{S r^2}{4 (d+d_o)^2} \qquad \frac{\text{neutrons}}{\text{second}}$$

where S is the source strength; r is the radius of the surface area A enclosed by the aperture; $d+d_o$ is the effective distance between the source and counter; α, the angle between the normal to the surface, A and the distance, $d+d_o$, is assumed small in final equation.

The efficiency of the counter is defined as the ratio of the number of neutrons counted per second to the number incident upon the counter face per second, that is

$$\varepsilon = \frac{CR}{N}$$

$$= \frac{4(CR)(d+d_o)^2}{S r^2} \qquad \frac{\text{counts}}{\text{incident neutron}}$$

where $\cos \alpha$ is assumed to be unity.

Neutron Sources and their Angular Distribution Corrections

Calibration of the long counter requires neutron sources that are monoenergetic and of known yield. Charged-particle reactions make available monoenergetic neutron sources if the ion beam itself is monoenergetic[9,11]. The $H^2(d,n)He^3$ and $H^3(d,n)He^4$ reactions have large reaction cross sections in the low energy range and are exoergic[14]. These two reactions provide high yields at low bombarding energies.

If the energetics of such reactions are considered, the following relation is obtained for the neutron

energy based upon the conservation laws for energy and momentum in the laboratory frame[14].

$$E_n^{1/2} = \frac{(M_d M_n E_d)^{1/2} \cos\theta}{M_n + M_r} \pm \left[\left\{ \frac{M_r - M_d}{M_n + M_r} + \frac{M_d M_n \cos^2\theta}{(M_n + M_r)^{1/2}} \right\} E_d + \frac{M_r}{M_n + M_r} Q \right]^{1/2}$$

where E_n and M_n are the energy and mass of the neutron respectively, E_d and M_d are the energy and mass of the deuteron respectively, M_r is the recoil particle mass, and θ is the emission angle of the neutron.

The angular distribution of the neutron yield for each of the above reactions is not isotropic in the laboratory frame, the degree of anisotropy varying with the bombarding deuteron energy. In the center-of-mass frame the angular distribution for a thick tritium target is isotropic in the region 15 Kev to 200 Kev[1,5] whereas the deuterium target is anisotropic in this same energy region[6].

As a consequence of the isotropic property in the center-of-mass frame for the $H^3(d,n)$ reaction, the

total yield per μ coulomb in the forementioned energy range can be expressed

$$Y(E) = 2\pi \int N(\theta') \sin\theta' d\theta'$$

$$= 4\pi N(\theta')$$

where $N(\theta')$ is the angular yield per μ coulomb per steradian[3,7]. To convert the above expression to the laboratory frame, the angular yields and their corresponding solid angles are equated, that is

$$\frac{N(\theta')}{N(\theta)} = \frac{d\Omega}{d\Omega'} = \frac{\sin\theta d\theta}{\sin\theta' d\theta'}$$

or $$N(\theta') = \left\{ \frac{\sin^3\theta}{\sin^3\theta'} \cdot (1 + \gamma\cos\theta') \right\} N(\theta)$$

The angular yield in the laboratory frame is expressed

$$N(\theta) = \frac{\sin^3\theta'}{\sin^3\theta} \left\{ \frac{1}{1 + \gamma\cos\theta'} \right\} \frac{Y(E)}{4\pi} \qquad \frac{\text{neutrons}}{\mu\text{coul-steradian}}$$

where γ is the ratio of the speed of the center-of-mass in the laboratory frame to the speed of the neutron in the center-of-mass frame[20].

In the $H^2(d,n)$ reaction, as a result of the anisotropy in the center-of-mass frame the angular distribution is given as

$$N(\theta') = N(90^\circ) \left\{ 1 + a(E) \cos^2 \theta' \right\} \quad \frac{\text{neutrons}}{\mu\text{coul-steradian}}$$

where $N(90^\circ)$ is the distribution of neutrons per μ coulomb per steradian at 90 degrees in the center-of-mass frame, a(E) is an asymmetry coefficient[6]. With this correction for anisotropy, the total yield for this reaction is obtained in a similar manner as described above.

Count Rate as a Function of Neutron Flux

To monitor fast neutron fluxes with the long counter, it is assumed that a single (n,α) reaction produces one count. The fast flux at the counter for a particular count rate, CR, is expressed

$$\phi = \frac{CR}{\varepsilon A}$$

where A is the area of the inner face and ε is the long counter efficiency.

REVIEW OF LITERATURE

The neutrons associated with the long counter can be classified into two energy groups. The incident beam of neutrons impinging upon the face of the counter is considered to constitute a fast energy group. After degradation in the paraffin, a second group of neutrons of thermal energy is considered since those neutrons primarily absorbed in the BF_3 detector are thermal neutrons. Such a two-group diffusion model is used by Kushneriuk[13] to investigate theoretically the efficiency of the long counter.

This approach requires a knowledge of the fast and thermal neutron density distributions within the counter since the fast group serves as the source for the thermal group. Using the incident neutron beam as the source for the fast neutron distribution in the counter, Kushneriuk writes the diffusion equation for the fast group as

$$\left[\nabla^2 - \frac{1}{L_s^2} \right] \varphi_f(r,z) = -q(r,z)$$

where $\rho_f(r,z)$ is the fast neutron density distribution, L_s is the slowing down length in paraffin, and $q(r,z)$ is the fast neutron source density. The effect of the presence of the BF_3 detector is neglected in determining the fast neutron density distribution.

The diffusion equation for the thermal neutron density distribution is expressed

$$\left[\nabla^2 - \frac{1}{L^2}\right] \rho_t(r,z) = -\frac{\tau}{L^2 \tau_f} \rho_f(r,z)$$

where $\rho_t(r,z)$ is the thermal neutron density distribution, τ is the mean life of a thermal neutron, τ_f is the mean life of a fast neutron, and L is the diffusion length. Again the presence of the BF_3 detector is neglected, giving rise to an unperturbed thermal distribution, $\rho_t(r,z)$; however, the (n,α) reaction with boron causes a flux depression directly outside the detector. As a consequence of this effect, Kushneriuk evaluates the counter efficiency in terms of both a perturbed and unperturbed thermal density distribution. The unperturbed thermal distribution is utilized for weakly absorbing detectors.

The validity of the expression derived by Kushneriuk for the efficiency of the long counter, shielded (outer paraffin and boron-trioxide layers) and unshielded, is observed in his plot of the counter efficiency versus the incident neutron energy.

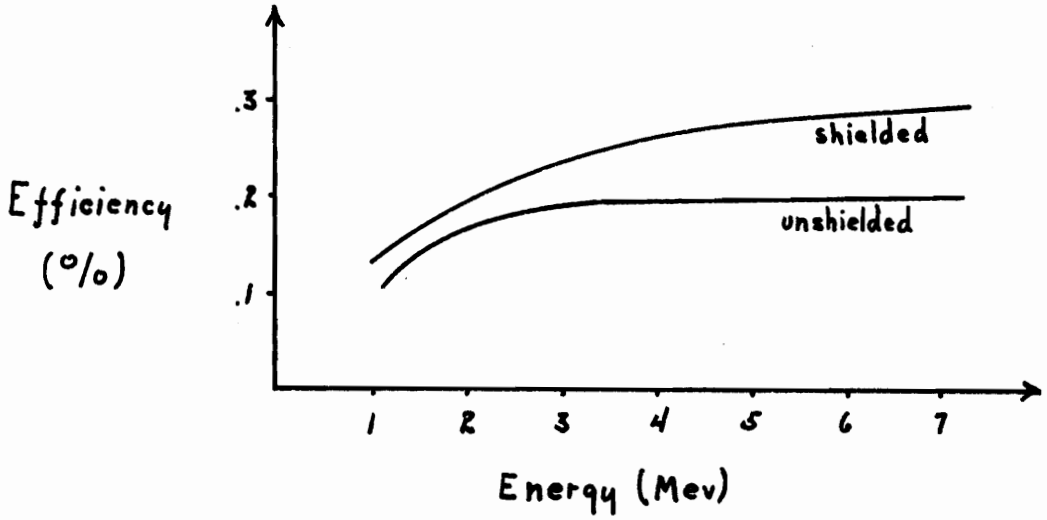

Hanson and McKibben[10] report from experimental observation that for the shielded counter, the efficiency is considerably increased for higher energy neutrons due to the larger mass of paraffin in the shield while the efficiency for low energy neutrons is relatively low.

In a closer examination of the response of the long counter Nobles et al.[15] observed fluctuations in the

counter efficiency of 5%. An investigation by this group using a (p,n) reaction on tritium reveals irregularities in the neutron yield at neutron energies of 2.08 Mev and 2.99 Mev. These anomalies are attributed to the occurrence of two prominent resonances in the total cross section of carbon at the same forementioned energies.

At Harwell, Allen[2] has published results of the response for a shielded long counter constructed with dimensions specified by Hanson and McKibben[10]. His results confirm the flatness of counter response over the range 25 Kev to 2 Mev.

APPARATUS

Long Counter Design

The shielded long counter consists of a cylinder of paraffin 8 inches in diameter surrounded by a 1/2 inch layer of B_2O_3 (anhydrous boric acid, Fisher) and an additional 3 inch layer of paraffin. (Calculations by Kushneriuk[13] indicate that this paraffin shield provides sufficient thickness to slow down neutrons of energies up to 10 Mev.) The entire paraffin arrangement is enclosed by a sheet metal shell of 40 mils thickness. Design dimensions for the long counter are illustrated in figure 1.

BF_3 Detectors

Boron-trifloride detector tubes of diameters 1 or 1/2 inch are used interchangeably with the counter as shown in figure 2. The smaller diameter BF_3 tube is supported in the center of a 1 inch diameter aluminum cylinder by means of paraffin. This unit is fitted within the 1 inch axial hole of the counter. Design specifications for each BF_3 tube are:

1/2 inch--

operating potential: 1500 volts

pressure: 40 cm of Hg

active length: 10.5 inches

manufacturer: N. Wood Counter Laboratories

1 inch (tube 909)--

operating potential: 4000 volts

pressure: 120 cm of Hg

active length: 6 inches

manufacturer: Radiation Counter Laboratories

Mounting the Long Counter

The long counter mounting consists of a table frame supporting an elevated platform on which the long counter is placed. This arrangement provides vertical adjustment of the counter from 56 to 85 inches from floor level as well as rotational movement of the supporting platform in a horizontal plane through 360 degrees. In addition, the counter axis can be rotated to an angle of 30 degrees with the horizontal plane of the supporting platform as shown in figure 3.

The table frame is constructed of 3/16 inch x 1 1/2 inches x 1 1/2 inches angle iron. For mobility of this

unit, 125 pounds "all directional" truck casters are attached to the frame. Design dimensions are shown in figure 4.

The counter platform, figure 5, is made of two 1/2 inch steel plates. These plates are hinged together such that at a distance of 3 inches apart, they are parallel. This separation allows the upper plate to be rotated upward to a maximum angle of 30 degrees with the lower plate. The counter is positioned on the upper plate by six pieces of angle iron beveled at 45 degrees. This unit is attached to the table frame by securing the lower plate to a length of 1 inch pipe which is fitted into a 1 1/2 inch pipe. The 1 1/2 inch pipe is secured to the table frame by two 3 inch steel channels illustrated in figure 4. This telescopic arrangement is locked in position by a collar. The 1 inch pipe turns freely within the 1 1/2 inch pipe, allowing the elevated platform to be rotated through 360 degrees.

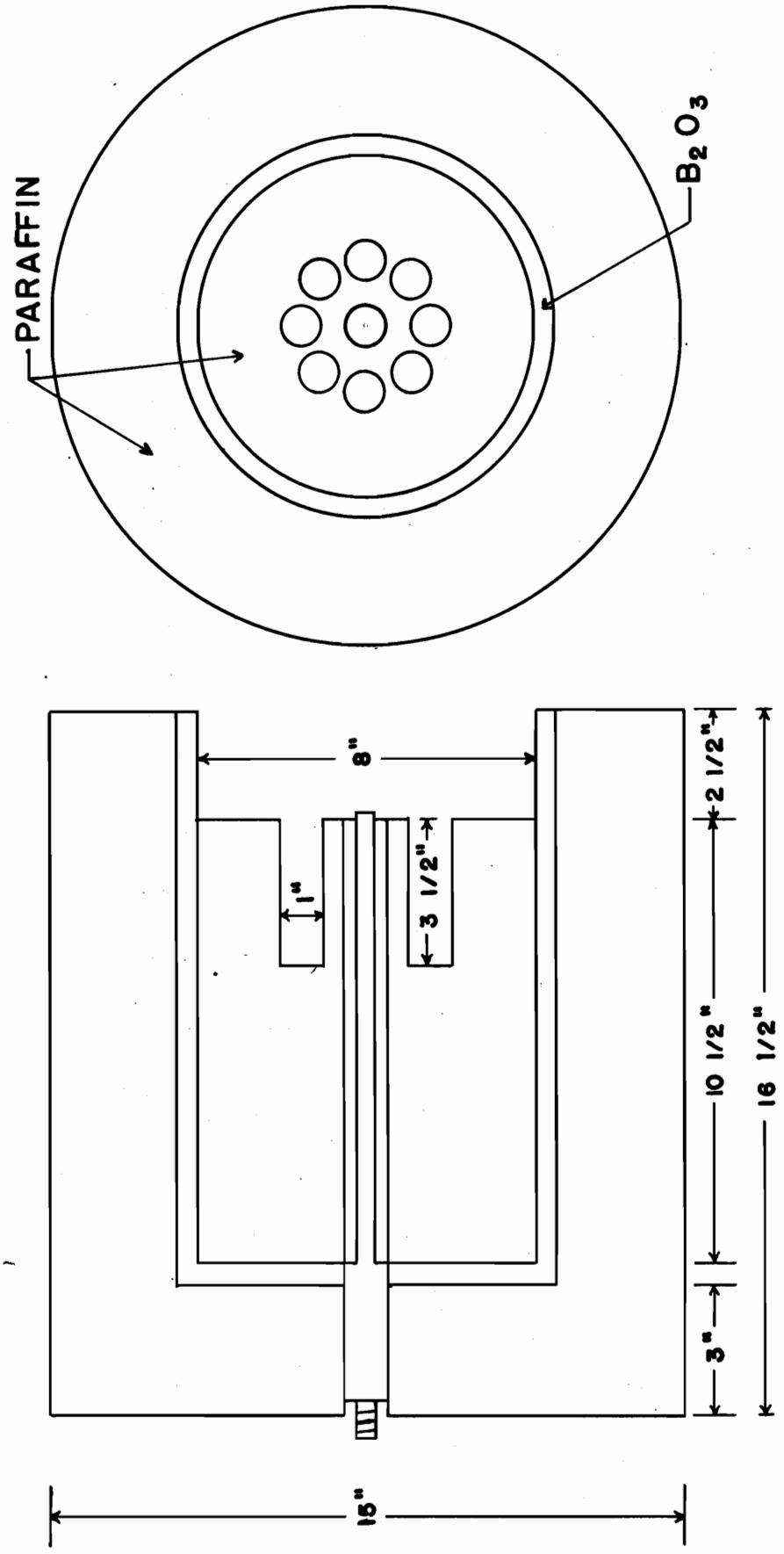

FIG. 1 LONG COUNTER

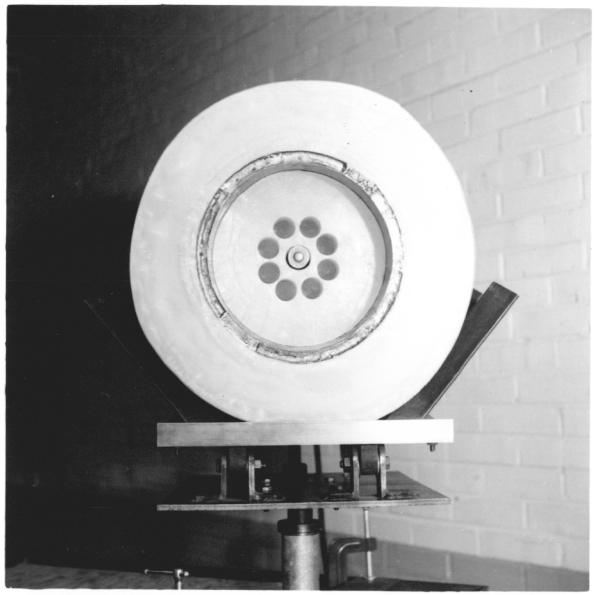

1/2" DIA. BF_3 TUBE

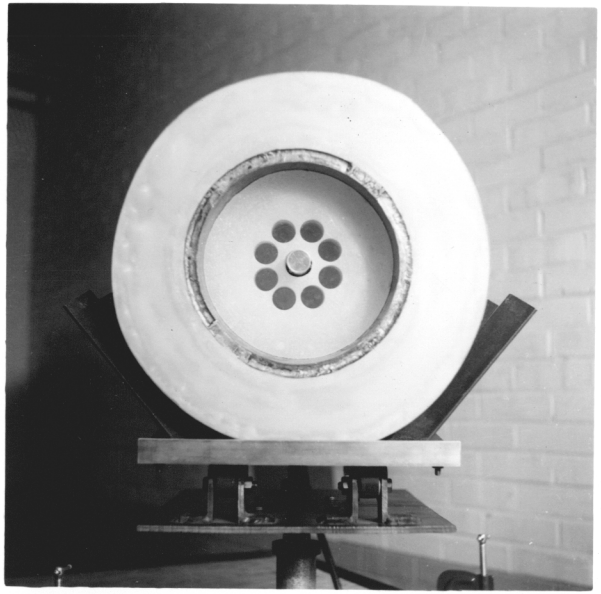

1" DIA. BF_3 TUBE

FIG. 2 POSITION OF BF_3 DETECTORS IN LONG COUNTER

FIG. 3 LONG COUNTER IN HORIZONTAL AND ROTATED POSITIONS

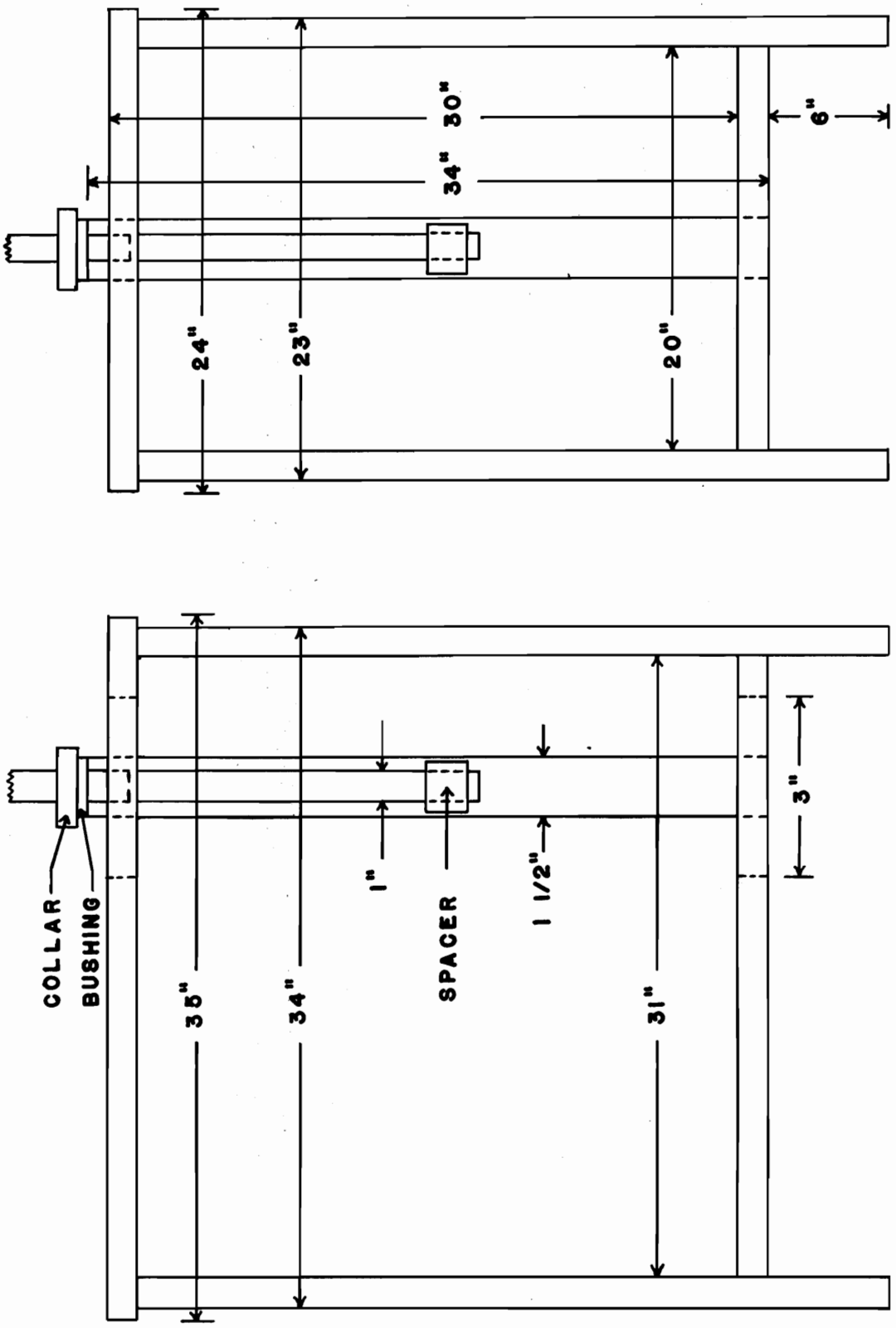

FIG. 4 TABLE FRAME

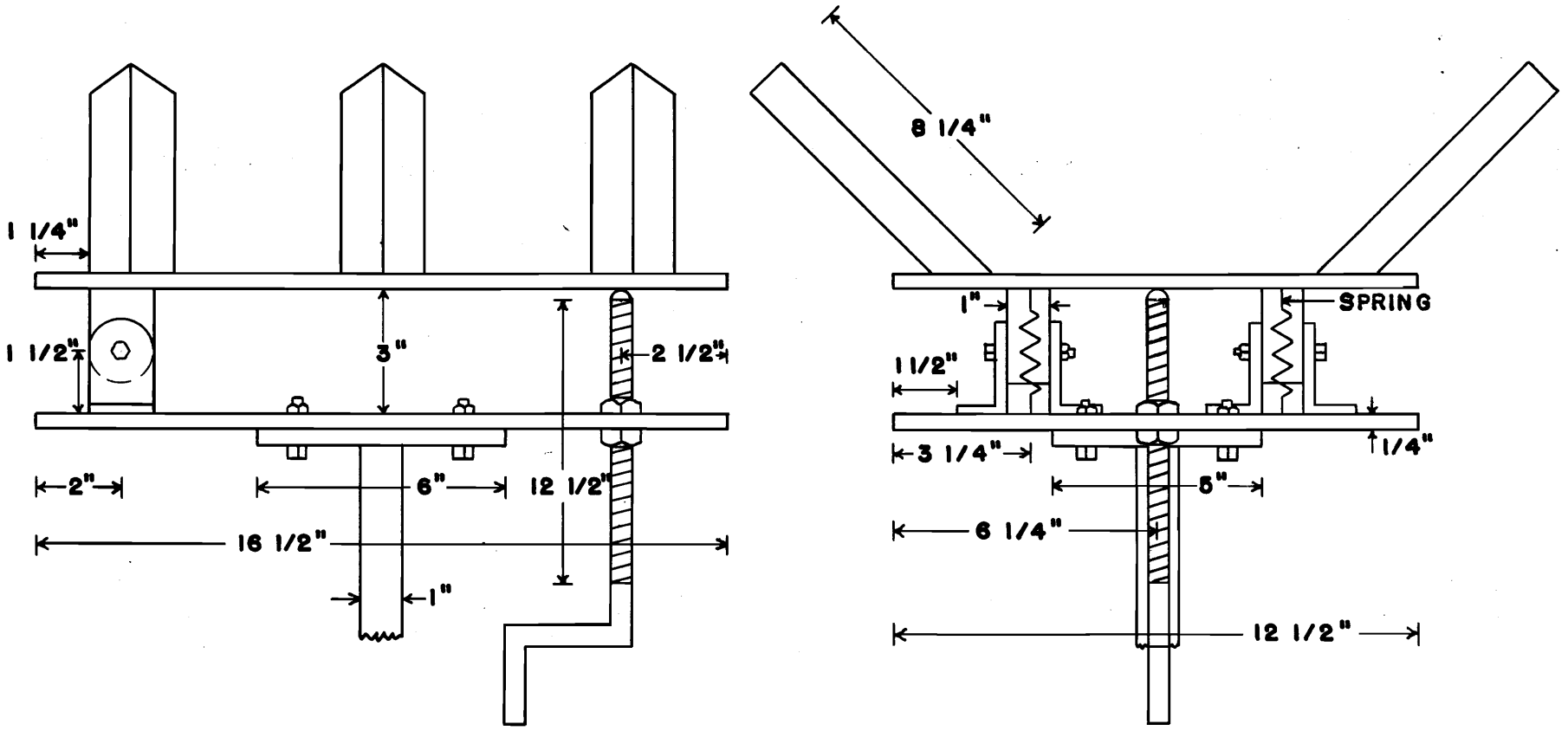

FIG. 5 ELEVATED PLATFORM

EXPERIMENTAL PROCEDURE

Arrangement of Counter and Neutron Sources

To minimize the contribution from wall scattering, the long counter and neutron source are placed in the center of a vacant room where both are elevated at best to a distance midway between the floor and ceiling. This arrangement is used for data with a plutonium-beryllium source. The source-counter height is 59 inches from floor level. The deuterium and tritium targets are 48 inches from the floor; this height is several inches lower than that which can be obtained by the counter. Consequently, the counter is adjusted such that the face of the counter is normal to the line of sight from the source to the counter. The presence of a large tank of water behind the deuterium and tritium targets causes a scattering effect which is reduced by enclosing the sides of the tank with cadmium. The position of the tank necessitates observation of the neutron yield at 90 degrees to the incident beam.

Evaluation of Penetration Depth

To obtain data for the determination of the effective center of the long counter, count rates are observed for source counter distances ranging from 20 to 100 inches. These distances are measured from the center of the source to the surface of the recessed face. Large counting rates are recorded to reduce statistical error.

Counting Procedure

Fluctuations in the beam current incident upon the deuterium and tritium targets produce deviations in count rates. To minimize this effect visual current monitoring is made for each measurement. Count rate variations are monitored further with the use of a BF_3 detector in a water moderator. (Standard deviations are associated with all count rates.)

Gamma pulses are discriminated against by adjusting the pulse height sensitivity of the counting circuit.

DISCUSSION OF RESULTS

Plutonium-Beryllium Neutron Source

The distribution of neutron energies for the plutonium-beryllium source ranges from 1 to 10 Mev with a broad peak in the spectrum occurring at 4 Mev[8]. The mean neutron energy for this source is estimated to be 3 to 4 Mev. The penetration depth for this average energy is established from the intercept of figure 6. This point is determined by the slope of that portion of the curve in the range 20 to 40 inches. The contribution of wall scattering within this range is not as noticeable as in the range 60 to 100 inches as illustrated by the curvature of the graphs.

As a consequence of the wall scattering effect, the mean counter efficiency, ϵ , is computed from data of table 2 in the source-counter range, 20 to 40 inches. The theoretical calculations of Kushneriuk[13] for a shielded long counter of similar dimensions give a counter efficiency of 0.24% as compared to 0.19% established in this thesis. Results published by Nobles et al.[15] yields a counter sensitivity of 5.6×10^{-6} counts per source neutron at a source-counter

distance of 41.5 inches compared to the 4.2×10^{-6} counts per source neutron at 40 inches for this thesis. The discrepancies in these comparisons are attributed to a pulse discrimination of 2 millivolts.

The mean counter efficiency with the 1 inch BF_3 detector in the counter is computed from values of table 1 over the same range, 20 to 40 inches. This value is 6.18×10^{-3} counts per incident neutron. (There exists no published data for comparison with this counter sensitivity.)

$H^3(d,n)He^4$ Reaction

As in the preceding results, the $H^3(d,n)$ reaction shows a departure from linearity in the curves of figure 7 for source counter distances greater than 40 inches. Counter efficiencies obtained for the 14.1 Mev neutrons from this source are computed from the data of tables 3 and 4 in the source-counter range, 30 to 40 inches. For the 1 inch BF_3 detector, the mean counter efficiency is 3.96×10^{-3} counts per incident neutron; whereas for the 1/2 inch BF_3 detector, this value is 1.00×10^{-3} counts per incident neutron.

Barchall et al.[4] have reported the efficiency for the shielded long counter to decrease to 67% for 14 Mev

neutrons. The results of this thesis yield a 64% decrease using the 1 inch diameter BF_3 tube, whereas the 1/2 inch diameter tube gives a 53% decrease.

$H^2(d,n)He^3$ Reaction

For the $H^2(d,n)$ reaction a deuterium drive-in target is used as a neutron source. The angular neutron yield for this source is not available; consequently, the source is not used for calibration. The total yield is predicted by other experimenters[18] to be of the order of 10^7 neutrons per second. Calculations, based upon the efficiency of the long counter determined with the plutonium-beryllium source, are made for the total yield with the assumption that the observation angle, 90 degrees, is the same in the center-of-mass frame. These computations, recorded in tables 5 and 6, give an average total neutron yield of 1.015×10^7 neutrons per second for a bombarding energy of 180 kv.

The Long Counter as a Fast Flux Monitor

To avoid the wall scattering effect, fast neutron fluxes, recorded in table 7, are computed from values of the count rate obtained in the source-counter range,

20 to 40 inches. Figure 9 illustrates the fast flux behavior as a function of count rate.

Table 1

Source: Plutonium-beryllium

Source strength: 1.6×10^6 neutrons per second

Detector: 1" diameter BF_3 tube

CR	$(CR)^{-1/2}$	$(d+d_o)$	ε
4400 ± 33	0.0151 ± 0.00006	20 + 3.1	6.11×10^{-3}
2133 ± 16	0.0216 ± 0.00008	30 + 3.1	6.08×10^{-3}
1307 ± 10	0.0277 ± 0.00011	40 + 3.1	6.34×10^{-3}
624 ± 6	0.0400 ± 0.00019	60 + 3.1	6.46×10^{-3}
403 ± 4	0.0497 ± 0.00025	80 + 3.1	7.20×10^{-3}
284 ± 3	0.0593 ± 0.00031	100 + 3.1	7.81×10^{-3}

where: CR = counts per minute

$(CR)^{-1/2}$ = (counts per second)$^{-1/2}$

$d+d_o$ = inches

ε = counts per incident neutron

Table 2

Source: Plutonium-beryllium

Source strength: 1.6×10^6 neutrons per second

Detector: 1/2" diameter BF_3 tube

CR	$(CR)^{-1/2}$	$(d+d_o)$	ε
1337 ± 12	0.0273 ± 0.00012	20 + 3.1	1.86×10^{-3}
660 ± 7	0.0389 ± 0.00021	30 + 3.1	1.88×10^{-3}
404 ± 4	0.0498 ± 0.00025	40 + 3.1	1.96×10^{-3}
189 ± 3	0.0727 ± 0.00058	60 + 3.1	1.97×10^{-3}
124 ± 2	0.0898 ± 0.00072	80 + 3.1	2.23×10^{-3}

FIG. 6
NEUTRON PENETRATION

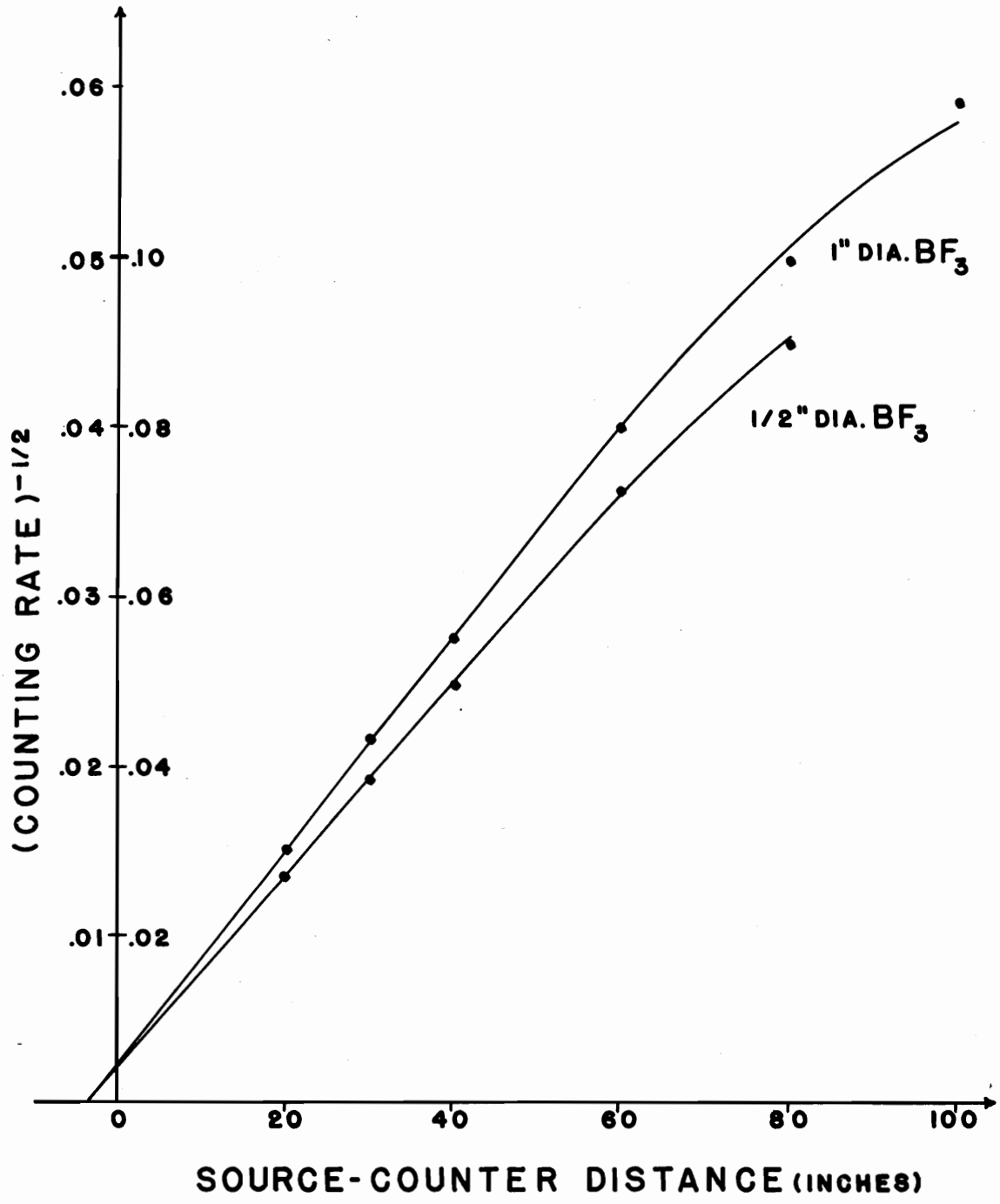

PENETRATION DEPTH: 3.1 INCHES
NEUTRON ENERGY: 4.0 MEV
SOURCE: Pu-Be

Table 3

Source: $H^3(d,n)He^4$ (tritium absorbed in zirconium)

Neutron yield: 1.2×10^6 neut./μ coul-steradian at 90° for E_d = 90 kv

Beam current: 10 μ amps

Detector: 1" diameter BF_3 tube

CR	$(CR)^{-1/2}$	$d+d_o$	ε
110982 ± 235	0.0030 ± 0.000003	30 + 6.1	3.98×10^{-3}
85263 ± 207	0.0034 ± 0.000004	35 + 6.1	3.95×10^{-3}
67616 ± 184	0.0038 ± 0.000005	40 + 6.1	3.94×10^{-3}
59082 ± 172	0.0041 ± 0.000006	45 + 6.1	4.38×10^{-3}
41847 ± 145	0.0049 ± 0.000008	50 + 6.1	3.58×10^{-3}

where: CR = counts per minute

$(CR)^{-1/2}$ = (counts per second)$^{-1/2}$

$d+d_o$ = inches

ε = counts per incident neutron

Table 4

Source: $H^3(d,n)He^4$ (tritium absorbed in zirconium)

Neutron yield: 1.2×10^6 neut./μ coul-steradian at 90° for E_d = 90 kv

Beam current: 10 μ amps

Detector: 1/2" diameter BF_3 tube

CR	$(CR)^{-1/2}$	$d+d_o$	ε
27894 ± 118	0.0060 ± 0.000013	30 + 6.1	0.99×10^{-3}
21686 ± 104	0.0068 ± 0.000016	35 + 6.1	1.00×10^{-3}
17420 ± 93	0.0076 ± 0.000020	40 + 6.1	1.02×10^{-3}
15272 ± 87	0.0081 ± 0.000023	45 + 6.1	1.13×10^{-3}
11774 ± 77	0.0092 ± 0.000030	50 + 6.1	1.01×10^{-3}

FIG. 7
NEUTRON PENETRATION

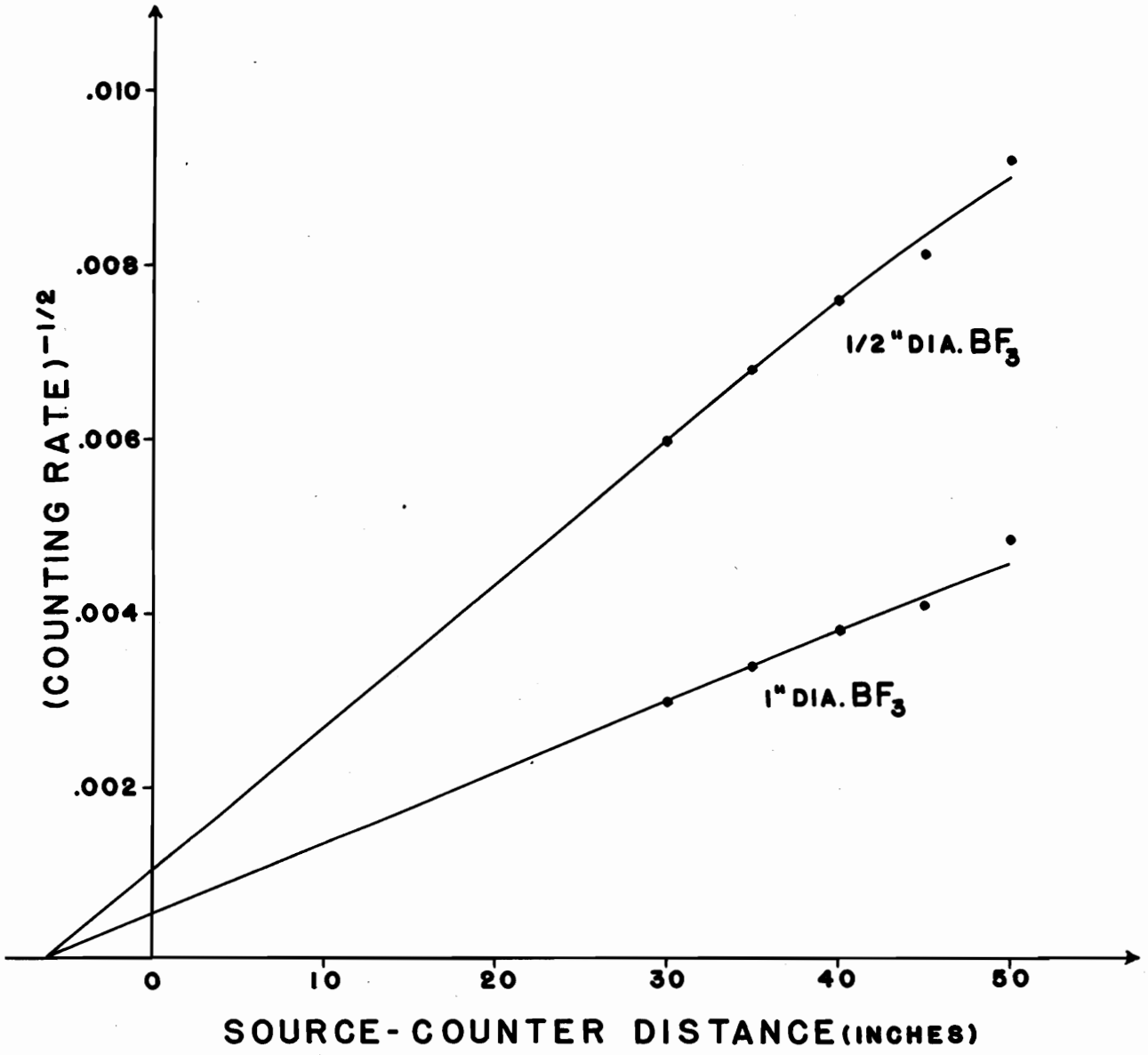

PENETRATION DEPTH: 6.1 INCHES
NEUTRON ENERGY: 14.1 MEV
SOURCE: $H^3(D,N)He^4$

Table 5

Source: $H^2(d,n)He^3$ (drive in target on brass backing)

Beam current: 100 μ amps at 180 kv

Detector: 1" diameter BF_3 tube

CR	$(CR)^{-1/2}$	$d+d_o$
14689 ± 60	0.0082 ± 0.000017	26 + 1.5
11342 ± 53	0.0094 ± 0.000022	30 + 1.5
8703 ± 47	0.0107 ± 0.000029	35 + 1.5
5968 ± 39	0.0129 ± 0.000042	40 + 1.5
5883 ± 38	0.0130 ± 0.000042	45 + 1.5
4315 ± 35	0.0152 ± 0.000062	50 + 1.5

where: CR = counts per minute

$(CR)^{-1/2}$ = (counts per second)$^{-1/2}$

$d+d_o$ = inches

$$Y(E)_{1"} = 9.30 \times 10^4 \frac{\text{neutrons}}{\mu \text{ coulomb}}$$

Table 6

Source: $H^2(d,n)He^3$ (drive in target on brass backing)

Beam current: 103 μ amps at 180 kv

Detector: 1/2" diameter BF_3 tube

CR	$(CR)^{-1/2}$	$d+d_o$
5221 ± 52	0.0138 ± 0.000069	26 + 1.5
3963 ± 44	0.0159 ± 0.000088	30 + 1.5
2997 ± 27	0.0183 ± 0.000082	35 + 1.5
2405 ± 24	0.0204 ± 0.00010	40 + 1.5
1973 ± 18	0.0225 ± 0.00010	45 + 1.5
1593 ± 16	0.0251 ± 0.00013	50 + 1.5

$$Y(E)_{1/2"} = 1.10 \times 10^5 \frac{\text{neutrons}}{\mu \text{ coulomb}}$$

FIG. 8
NEUTRON PENETRATION

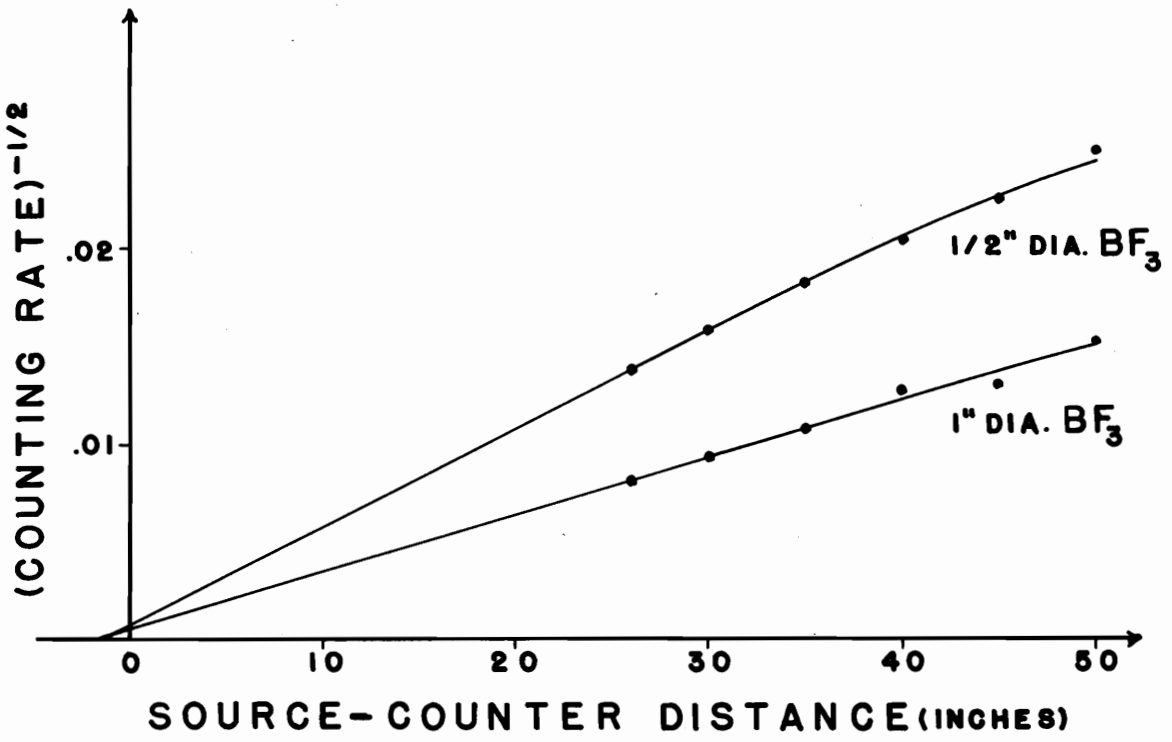

PENETRATION DEPTH: 1.5 INCHES
NEUTRON ENERGY: 2.5 MEV
SOURCE: $H^2(D,N)He^3$

Table 7

Sources	Source-Counter Distance	CR(1" dia. BF_3)	CR(1/2" dia. BF_3)	ϕ
Pu-Be	20"	73.3	22.3	36.45
Pu-Be	30"	35.6	11.0	17.85
Pu-Be	40"	21.8	6.7	10.45
$H^2(d,n)He^3$	30"	189.0	66.0	100.85
$H^2(d,n)He^3$	40"	99.5	40.1	57.50
$H^3(d,n)He^4$	35"	1421.0	361.4	1111.05
$H^3(d,n)He^4$	40"	1126.9	290.3	885.65

where: CR = counts per second

ϕ = neutrons/cm^2-second

FIG. 9
EVALUATION OF FAST FLUX

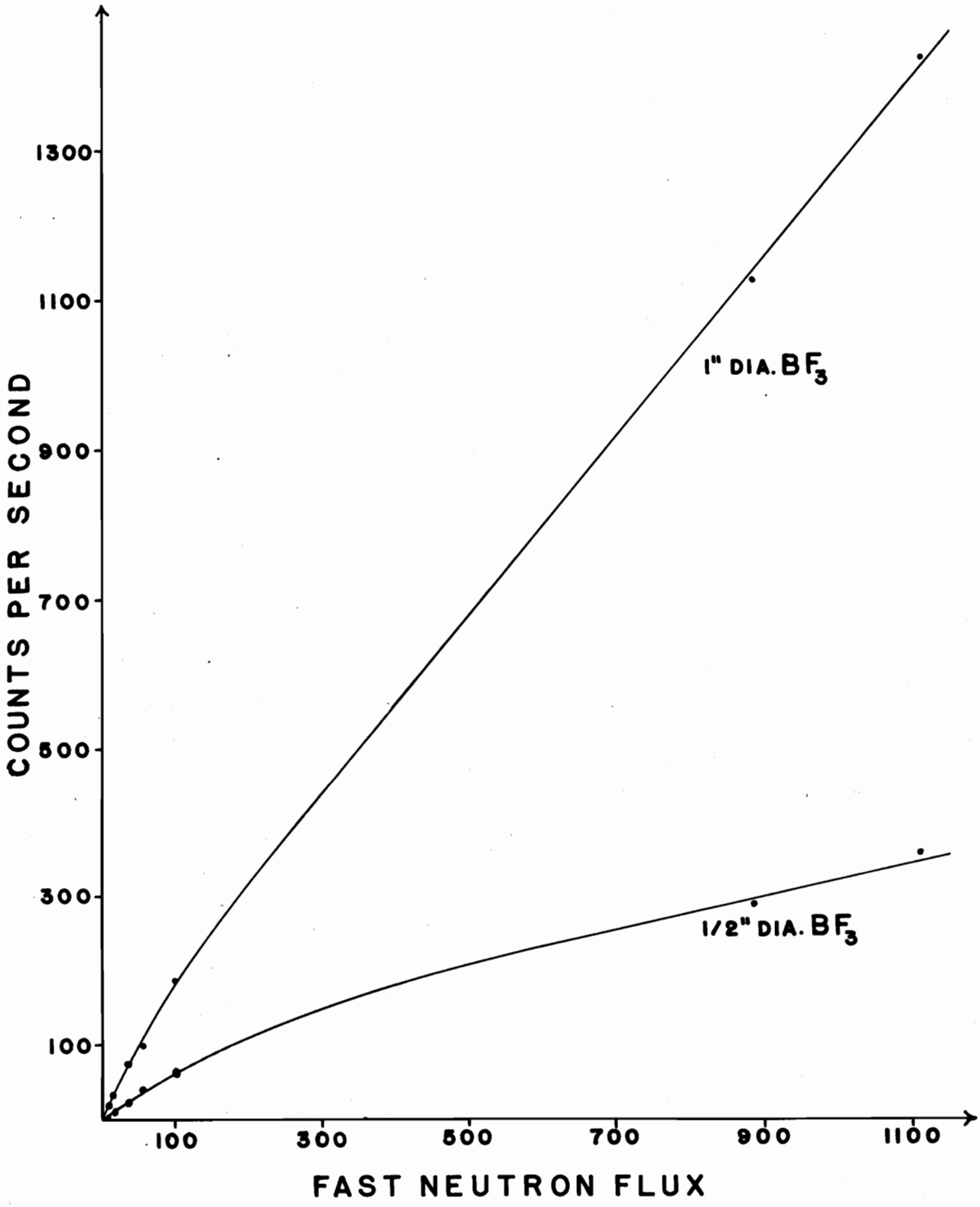

SUMMARY

A BF_3 fast neutron dosimeter has been designed and constructed similar to the shielded long counter reported by Hanson and McKibben[10]. Calibration of the dosimeter with a plutonium-beryllium source and the $H^3(d,n)He^4$ reaction has given rise to the following counter efficiencies in the source-counter range, 20 to 40 inches:

1" dia. BF_3 tube:

$\varepsilon = 6.18 \times 10^{-3}$ count per incident 4.0 Mev neutron

$\varepsilon = 3.96 \times 10^{-3}$ count per incident 14.1 Mev neutron

1/2" dia. BF_3 tube:

$\varepsilon = 1.90 \times 10^{-3}$ count per incident 4.0 Mev neutron

$\varepsilon = 1.00 \times 10^{-3}$ count per incident 14.1 Mev neutron

For the purposes of neutron dosimetry, the fast neutron flux has been expressed as a function of the count rate of the long counter. In figure 9, these results have been plotted.

ACKNOWLEDGMENTS

The author wishes to express his gratitude to Dr. Andrew Robeson for his guidance and generous advice during this project. Also, he desires to express his appreciation to Mr. Luther Barnett for his advice and assistance in the construction of the support for the long counter. Since the use of the Cockcroft-Walton accelerator requires group effort, it is with appreciation that the author thanks those students of the graduate school who assisted in this capacity.

A word of thanks is extended to the parents of the author for their support and encouragement throughout this project.

BIBLIOGRAPHY

1. Allan, D. L. and Poole, M. J., Proceedings of the Royal Society (London), A 204,500 (1950)
2. Allen, W. D., Atomic Energy Research Establishment (England), NP/R 1667, 1 (1955)
3. Arnold, W. R., Phillips, J. A., et al., Physical Review 93, 483 (1954)
4. Barschall, H. H., Rosen, L., and Taschek, R. F., Reviews of Modern Physics 24, 1 (1952)
5. Bretscher, E. and French, A. P., Physical Review 75, 1154 (1949)
6. Bretscher, E., French, A. P., and Seidl, F. G. P., Physical Review 73, 815 (1948)
7. Conner, J. P., Bonner, T. W., and Smith, J. R., Physical Review 88, 468 (1952)
8. Curtiss, L. F., Introduction to Neutron Physics, p. 93, D. Van Nostrand Company, Inc., New York, 1959
9. Fowler, J. L. and Bralley, J. E., Reviews of Modern Physics 28, 103 (1956)
10. Hanson, A. O. and McKibben, J. L., Physical Review 72, 673 (1947)

11. Hanson, A. O., Taschek, R. F., and Williams, J. H., Review of Modern Physics 21, 635 (1949)

12. Jaffey, A. H., Review of Scientific Instruments 25, 349 (1954)

13. Kushneriuk, S. A., Canadian Journal of Physics 30, 402 (1952)

14. Mather, K. B. and Swan, P., Nuclear Scattering, p. 129, Cambridge University Press, London, 1958

15. Nobles, R. A., Day, R. B., et al., Review of Scientific Instruments 25, 334 (1954)

16. Price, W. J., Nuclear Radiation Detection, p. 38, McGraw-Hill Book Company, Inc., New York, 1958

17. ibid, p. 260

18. Robeson, A., Private Communication

19. Rossi, B. B. and Staub, H. H., Ionization Chambers and Counters, p. 192, McGraw-Hill Book Company, Inc., New York, 1949

20. Schiff, L. I., Quantum Mechanics, p. 99, McGraw-Hill Book Company, Inc., New York, 1949

VITA

The author was born September 11, 1936, in Newport News, Virginia. He received his elementary and secondary education in the Newport News public schools, Newport News, Virginia. In 1958 he received his B. S. degree in physics from the College of William and Mary, Williamsburg, Virginia. He enrolled in Virginia Polytechnic Institute and began his M. S. program in physics in September, 1958.

Walter Alfred Leyland Jr.

Walter Alfred Leyland, Jr.

ABSTRACT

A BF_3 fast neutron dosimeter or long counter is constructed and calibrated for use with the Cockcroft-Walton accelerator and UTR-10 reactor at Virginia Polytechnic Institute. The counter consists of a paraffin cylinder 8 inches in diameter, having a BF_3 proportional detector on the axis and a set of holes around the detector to improve the low energy response. External shields of paraffin, 3 inches thick, and boron-trioxide, 1/2 inch thick, enclose the paraffin cylinder. These shields serve to reduce the background effect and improve the high energy response.

Calibration of the counter is accomplished using as neutron sources: plutonium-beryllium and the induced reactions $H^2(d,n)He^3$ and $H^3(d,n)He^4$. Long counter efficiencies for both a 1 inch and 1/2 inch BF_3 tube yield a flat response over the energy range, 2.5 to 4 Mev whereas an approximately 60% decrease in efficiency is observed for a 14.1 Mev neutron.

Count rate of long counter is expressed as a function of the incident neutron flux. Neutron fluxes, ranging from 0 to 1100 neutrons/cm^2-second are monitored with the counter.